



HAL
open science

Tropical Wave Observations From the Reel-Down Atmospheric Temperature Sensor (RATS) in the Lowermost Stratosphere During Strateole-2

Martina Bramberger, Doug Goetz, M. Joan Alexander, Lars Kalnajs, Albert Hertzog, Aurelien Podglajen

► **To cite this version:**

Martina Bramberger, Doug Goetz, M. Joan Alexander, Lars Kalnajs, Albert Hertzog, et al.. Tropical Wave Observations From the Reel-Down Atmospheric Temperature Sensor (RATS) in the Lowermost Stratosphere During Strateole-2. *Geophysical Research Letters*, 2023, 50 (17), 10.1029/2023GL104711 . hal-04297087

HAL Id: hal-04297087

<https://hal.science/hal-04297087v1>

Submitted on 21 Nov 2023

HAL is a multi-disciplinary open access archive for the deposit and dissemination of scientific research documents, whether they are published or not. The documents may come from teaching and research institutions in France or abroad, or from public or private research centers.

L'archive ouverte pluridisciplinaire **HAL**, est destinée au dépôt et à la diffusion de documents scientifiques de niveau recherche, publiés ou non, émanant des établissements d'enseignement et de recherche français ou étrangers, des laboratoires publics ou privés.

1
2
3
4
5
6
7
8
9
10
11
12

Tropical wave observations from the Reel-down Atmospheric Temperature Sensor (RATS) in the lowermost stratosphere during Strateole-2

Martina Bramberger¹, Doug Goetz², M. Joan Alexander¹, Lars Kalnajs²,
Albert Hertzog³, Aurelien Podglajen³

¹NorthWest Research Associates, Boulder Office, Colorado, USA

²Laboratory for Atmospheric and Space Physics, University of Colorado, Boulder, CO, USA

³Laboratoire de Météorologie Dynamique, Ecole Polytechnique, Palaiseau, France

Key Points:

- high-resolution observations in the lowermost stratosphere from a new instrument
- Instrument detected tropical waves at resolution limit of reanalyses
- ERA5 reproduces waves, but temporal evolution differs from observations

Corresponding author: Martina Bramberger, martina@nwra.com

13 **Abstract**

14 Tropical waves play an important role in driving the quasi-biennial oscillation (QBO)
 15 of zonal winds in the tropical lower stratosphere. In our study we analyze these waves
 16 based on temperature observations from the 2021-2022 Strateole-2 campaign when the
 17 Reel-down Atmospheric Temperature Sensor (RATS) was successfully deployed for the
 18 first time. RATS provides long-duration, continuous and simultaneous high-resolution
 19 temperature observations at two altitudes (balloon float level and 200m below) allow-
 20 ing for an analysis of vertical wavelengths. This separation distance was chosen to fo-
 21 cus on waves near the resolution limit of reanalyses. Here, we found tropical waves with
 22 periods between about 6 hours and 2 days, with vertical wavelengths between 1.5 km and
 23 5 km, respectively. Comparing our results to ERA5 reanalyses we found good agreement
 24 for waves with a period longer than one day. However, the ERA5 amplitudes of high-
 25 frequency waves are under-estimated, and the temporal evolution of most wave packets
 26 differs from the observations.

27 **Plain Language Summary**

28 We present measurements from the maiden flight of the RATS instrument (Reel-
 29 down Atmospheric Temperature Sensor) in November/December 2021. The instrument
 30 lowered a temperature sensor down to about 200 m from a balloon floating at about 18 km.
 31 By combining the temperature measurements at balloon floating level and RATS we an-
 32 alyze tropical waves with relatively small vertical wavelengths (<6 km). These waves are
 33 important as they drive the quasi-biennial oscillation in the east-west winds in the trop-
 34 ical stratosphere. This oscillation is acknowledged as an important process for seasonal
 35 forecasts, but it is currently not well resolved in weather or seasonal forecast models. In
 36 our study we compare the observed waves with waves in one weather model system (ERA5)
 37 and find that the spectral energies are similar for long-period waves (>1 day). However,
 38 the high-frequency waves (that provide about 25% of the necessary QBO forcing) are
 39 under-estimated by ERA5, which is likely related to the limited vertical resolution.

40 **1 Introduction**

41 Strateole-2 is a French-US project with a focus on dynamics, microphysics and com-
 42 position in the tropical upper troposphere and lower stratosphere using long-duration
 43 superpressure balloons. Measurements include winds, temperatures, composition, clouds
 44 and aerosols from a variety of in situ and remote sensing instruments (Haase et al., 2018;
 45 Corcos et al., 2021; Kalnajs et al., 2021; Goetz et al., 2023). One goal is improved char-
 46 acterization of tropical waves, which drive variability in temperature and high cirrus clouds
 47 that have impacts on global stratospheric water vapor and decadal-scale climate vari-
 48 ability (J.-E. Kim et al., 2016; Jensen et al., 2017; Solomon et al., 2010)

49 Tropical waves also drive the Quasi-Biennial Oscillation (QBO) in lower stratospheric
 50 zonal winds, a circulation with notable impacts on long-range prediction (Scaife et al.,
 51 2022). Global model systems struggle to simulate these climate processes (Richter, Anstey,
 52 et al., 2020; Davis et al., 2017), likely in part due to poor resolution of the short hori-
 53 zontal and/or vertical scales of important tropical waves (Holt et al., 2020; Richter, Butchart,
 54 et al., 2020; J.-E. Kim & Alexander, 2015; Bramberger et al., 2022).

55 To study the effects of tropical waves on QBO and cirrus clouds, global reanaly-
 56 ses provided by different centers for numerical weather prediction have been widely used
 57 (Ern et al., 2014; Y.-H. Kim & Chun, 2015; Pahlavan, Fu, et al., 2021; Pahlavan, Wal-
 58 lace, et al., 2021; Ueyama et al., 2023). Due to its higher horizontal resolution compared
 59 to its predecessors, the fifth generation European Centre for Medium-Range Weather Fore-
 60 casts (ECMWF) Reanalysis (ERA5) is capable to resolve a wider spectrum of tropical

61 waves. This also allows for an improved representation of the wave-mean flow interac-
 62 tion which is crucial for the generation of the QBO (Pahlavan, Fu, et al., 2021).

63 Recently, balloon studies have shown the importance of very short vertical wave-
 64 length 1-5 day intrinsic period gravity waves with momentum fluxes that will contribute
 65 substantial forces to the QBO in the lower stratosphere (Vincent & Alexander, 2020; Bram-
 66 berger et al., 2022). These studies highlighted limitations of vertical resolution in reanal-
 67 yses for representing short-vertical scale tropical waves, even for the high ($\sim 350\text{m}$) res-
 68 olution of ERA5. Together with modeling studies these observations highlight the im-
 69 portance of high vertical resolution in the realistic representation of the QBO (Garfinkel
 70 et al., 2022).

71 Motivated by these results, Strateole-2 balloons equipped with specialized sensors
 72 were launched in the tropics in late 2021 with flight levels within the TTL and lower strato-
 73 sphere. A new measurement platform named the Reel-down Atmospheric Temperature
 74 Sensor (RATS), which senses temperature at the isopycnic balloon level and hundreds of
 75 meters below the balloon level had its maiden flight November-December 2021. The goal
 76 of these measurements is to characterize tropical waves in the short vertical wavelength
 77 range that straddles the limits of ERA5 resolution. For this study we use RATS data
 78 in conjunction with balloon level Thermodynamical SENSor (TSEN) observations (Hertzog
 79 et al., 2004) to characterize tropical waves near 18 km in the lowermost tropical strato-
 80 sphere. We use these unique measurements and ERA5 fields, to characterize tropical waves
 81 above the Indian Ocean in the lowermost tropical stratosphere and study their repre-
 82 sentation in ERA5.

83 2 Data and Instruments

84 2.1 Strateole-2 in situ TSEN observations

85 For Strateole-2, 25 super-pressure balloons were launched during two campaigns
 86 from the Seychelles. The first campaign took place from November 2019 to February 2020
 87 and the second campaign from October 2021 to January 2022. These balloons circum-
 88 navigate the equator at 18 km or 20 km (Haase et al., 2018; Corcos et al., 2021). We fo-
 89 cus on balloons C1-15-TTL4 (TTL4) and C1-16-TTL5 (TTL5) where both balloons are
 90 equipped with the TSEN temperature sensor at floating level (Hertzog et al., 2004) and
 91 the TTL5 balloon additionally carried the RATS instrument (see Fig. 1a). The TTL5
 92 super-pressure flight duration was approximately 42 days and RATS was operational for
 93 the first 16 days of the flight. Due to closely spaced launch times (< 2 hr) and near-identical
 94 float altitudes, the TTL4 and TTL5 balloons were floating in close proximity over the
 95 course of 10 days (see Fig. 1a and c). This permits combination of the in-situ observa-
 96 tions of these two balloons for the purpose of analyzing the horizontal wavelengths of
 97 tropical waves.

98 In-situ balloon observations of ambient temperature, pressure and horizontal wind
 99 vectors at the isopycnic floating levels of the Strateole-2 balloons were done with TSEN.
 100 Wind speeds are calculated from the GPS position of the drifting balloon gondola. The
 101 temperature sensor accuracy is 0.1 K at night and 0.25 K during the day after correction
 102 for solar radiation (Hertzog et al., 2004). The precision of TSEN temperatures is on av-
 103 erage about 4 mK for night-time measurements and about 20 mK for daytime, respec-
 104 tively (Wilson et al., 2023). The absolute accuracy and precision of the pressure sensor
 105 are ± 2 hPa and 0.01 hPa. Winds are derived from position with 0.1 ms^{-1} precision. The
 106 temporal resolution of this data set is 30 s.

107

2.2 RATS

108

109

110

111

112

113

114

115

116

117

118

119

120

121

122

123

124

125

126

127

RATS is a platform designed to make simultaneous, continuous and fast-response measurements of temperature, pressure, and position at two altitudes from a drifting high-altitude balloon using the TSEN temperature and GPS (Fig. 1b). The temperature sensors were separated vertically by a reel-down cable, with one TSEN at the "Euros" control gondola flight level and the other at the end of the reel-down cable. The lower sensor was attached to a suspended sub-gondola, or end-of-fiber-unit (EFU). For the TTL5 flight, the separation length was about 200 m, but other lengths are possible on future flights. The flight level gondola contained the data and communications interface of RATS in addition to the mechanical reeling system used to deploy the EFU, which is identical to the reel system used by the FLOATS instrument (Goetz et al., 2023). The EFU design and implementation was also identical to FLOATS, with the TSEN probe located on a thin white PTFE wire about 1 m below the EFU sub-gondola. Other specifications can be found in (Goetz et al., 2023). Additionally, the same 600 μm diameter liquid crystal polymer (LCP) coated fiber optic cable used for FLOATS was used to suspend the EFU. Its UV radiation exposure rating and breaking strain meet the International Civil Aviation Organization (ICAO) regulatory standards (i.e. Rules of the Air ICAO Appendix 4 Annex 2). For TTL5 the EFU was configured to transmit GPS position and TSEN pressure and temperature every 10 to 30 s via Long Range (LoRa) radio to the flight level gondola interface system. The Euros level TSEN and GPS was configured to a sampling period of 30 s and the EFU data was synced to the same clock.

128

2.3 ERA5 in Balloon Trajectory-Following Coordinates

129

130

131

132

133

ERA5 is an atmospheric reanalysis available at 6 hour intervals on 137 vertical levels up to 1hPa (Hersbach et al., 2020). The distance between the different vertical levels is about 400 m in the lower stratosphere and the horizontal resolution is 31 km. For this study the hourly ERA5 data was interpolated both in space and time to the balloon flight tracks of TTL4 and TTL5, respectively.

134

3 Methods

135

136

137

138

139

To determine the vertical or horizontal wavelengths we generally follow the approach of previous studies (Alexander et al., 2008; Wright et al., 2010; Ern et al., 2014; Alexander, 2015) who used adjacent satellite-borne temperature profiles to infer horizontal wavelengths. However for RATS analysis, we take into account covariance between two temperature time series rather than covariance between adjacent vertical profiles.

140

3.1 RATS vertical wavelength estimates

141

142

143

144

145

To calculate vertical wavelengths we use the temperatures measured with RATS (~ 200 m below balloon flight level) and TSEN (at balloon floating level) systems. We decompose the temperature observations into time t and frequency ω spectrum applying the Stockwell transform (Stockwell et al., 1996). The covariance between the two spectra C_{TR} can be written as

146

$$C_{TR}(t, \omega) = \hat{T}_t \hat{T}_r^* \quad (1)$$

147

148

149

where the \hat{T}_t and \hat{T}_r^* are the complex temperature amplitude spectra observed by TSEN at balloon level and by RATS ~ 200 m below the balloon, respectively. (See Fig.1b.) The star denotes the complex conjugate of \hat{T}_r . The phase shift is computed with

150

$$\Delta\phi_{TR} = \arctan\left(\frac{\text{Im}(C_{TR})}{\text{Re}(C_{TR})}\right) \quad (2)$$

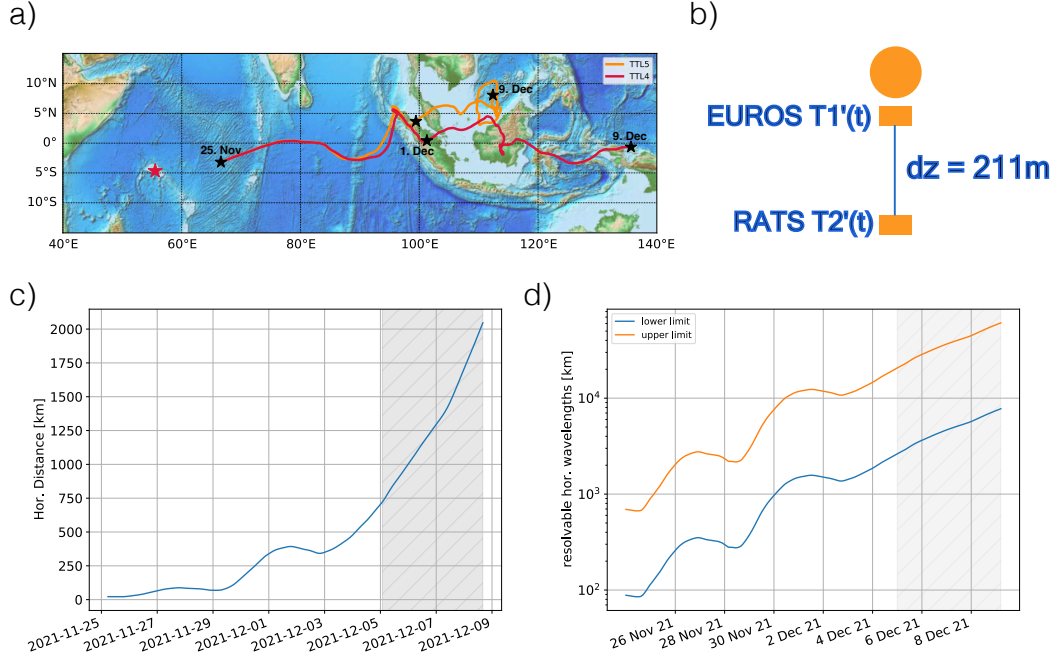


Figure 1. (a) Flight track of the TTL4 (red) and TTL5 (orange) balloons from 25th November to 9th December. The stars show the balloon positions on the 25th November, 1st December and 9th December, respectively. The red star highlights the Seychelles islands where the balloons were launched. (b) Schematic of TTL5 temperature measurements where RATS is on average 211m below the balloon. (c) Horizontal distance between the two balloons between 25th November and 9th December. (d) Theoretical upper and lower limits of horizontal wavelengths that can be resolved based on the horizontal distance of the balloons. Grey shading indicates the time period where the horizontal distance was too large and the data was excluded from the analysis.

151 From the vertical phase shift $\Delta\phi_{TR}$ and the vertical distance $\Delta_z = 211$ m we can then
 152 estimate the vertical wavelength

$$153 \quad \lambda_z = \frac{\Delta\phi_{TR}}{\Delta_z}. \quad (3)$$

154 Due to the sensitivity of the instrument and to avoid aliasing effects we define wave pack-
 155 ets with a covariance threshold $> 0.5 K^2$ and only compute vertical wavelengths where
 156 the observed phase difference $|\Delta\phi_{TR}|$ is in the range $0.2 - \pi$.

157 As the vertical distance between the RATS and balloon observed temperatures is
 158 a constant the resolvable vertical wavelengths range from ~ 420 m to 6.6 km throughout
 159 the observation period.

160 3.2 Dual-balloon horizontal wavelength estimates

161 As the balloons TTL4 and TTL5 were floating in close proximity over 10 days we
 162 can also estimate the horizontal wavelength λ_x analogous to the vertical wavelength. In
 163 this case the equation changes to

$$164 \quad \lambda_x = \frac{\Delta\phi_{45}}{\Delta_x(t)} \quad (4)$$

165 where $\Delta\phi_{45}$ is the phase shift derived from the co-spectral analysis of TTL4 and TTL5
 166 measured in-situ temperatures at the Euros gondola level and $\Delta_x(t)$ is the horizontal dis-
 167 tance between the two balloons which varies with time (see Fig.1c). As the horizontal

168 distance between the two balloons varies with time the resolvable horizontal wavelength
 169 range changes accordingly (see Fig.1d). Note, we limit the application of this method
 170 to times where Δ_x is smaller than 750 km and where the change in time of Δ_x is also
 171 small. Also note that compared to their horizontal separation, the mean vertical distance
 172 between the two balloons was negligibly small and is neglected in the analysis.

173 4 Results

174 4.1 Vertical and horizontal wavelength estimates from balloon obser- 175 vations

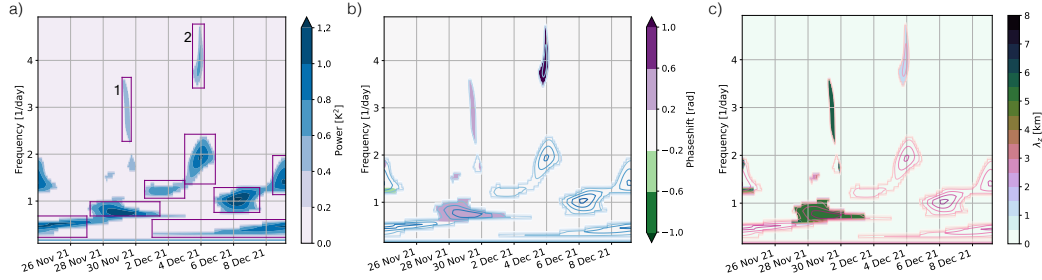


Figure 2. (a) Covariance of the temperatures measured by RATS and TSEN with a mask to only show significant amplitudes (power $> 0.5K^2$). (b) Phase shift for significant wave packets with overlain covariance contours for reference. (c) Vertical wavelength for wave packets with detectable signals (where phase shift > 0.2 radians). All spectra are shown as a function of time and wave frequency.

176 The covariance calculated from RATS and balloon flight-level observed tempera-
 177 tures shows enhanced power for waves with periods between 12 hours and 2.5 days be-
 178 tween 25th November 2021 and 8th December 2021 (Fig. 2a). Boxes on the figure iden-
 179 tify potential candidate wave packets for analysis. The corresponding phase shifts, com-
 180 puted as amplitude-weighted averages for each packet, reveal two high-frequency waves
 181 and one low-frequency wave packet with detectable phase shifts in these measurements
 182 (Fig. 2b). For these wave packets the vertical wavelengths range from 1.5 km to 5.5 km
 183 (Fig. 2c). For wave packets with a vertical wavelength larger than 6.6 km the phase shift
 184 becomes so small that it cannot be detected with the deployed instrument configuration.

185 Over the course of 10 days the balloons TTL4 and TTL5 floated in close proxim-
 186 ity ($\Delta x < 750$ km) allowing the analysis of horizontal wavelengths (see Fig. 3). Again the
 187 covariance shows wave packet signals for periods between 5 hours and 2 days and phase
 188 shifts are detectable (> 0.2) especially for wave packets after 30 November 2021. The es-
 189 timated horizontal wavelengths range between 500 km and 3000 km (see Fig. 3c). Note,
 190 that the horizontal distance between the two balloons varies with time (see Fig. 1a and
 191 c) which means that changes in the derived horizontal wavelengths over a wave packet
 192 could be related to the change of horizontal distance between the balloons with time if
 193 the wavelength shifts in or out of the observable range (see Eq.4 and Fig.1d).

194 4.2 Comparison to ERA5 reanalyses

195 As a next step we compare the observed covariances with ERA5 temperature cov-
 196 ariances. For the comparison with the vertical RATS-TTL5 covariances we choose the
 197 two ERA5 model levels that are closest to the balloon and RATS floating level. Please
 198 note that the vertical grid spacing of ERA5 at this altitude region is about 350 m whereas

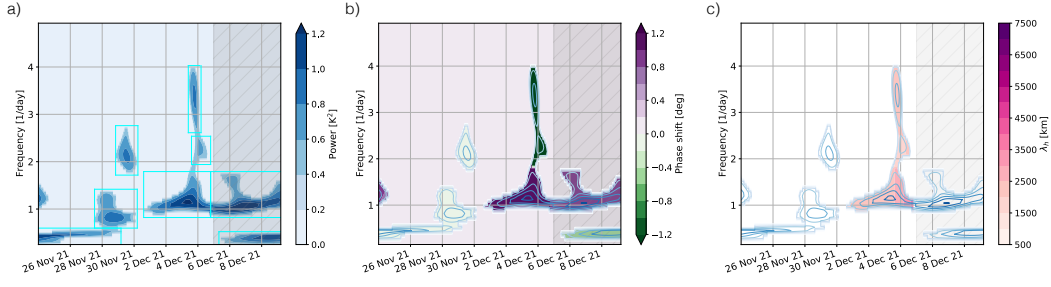


Figure 3. (a) Covariance of the temperatures measured by TTL4 and TTL5 TSEN with a mask to only show significant amplitudes (power $> 0.5K^2$). (b) Phase shift between the temperatures for significant wave packets. (c) Resulting horizontal wavelength for significant wave packets and phase shift > 0.2 radians. All spectra are shown as a function of time and wave frequency. Grey shaded areas highlight the time where the horizontal distance exceeds the threshold.

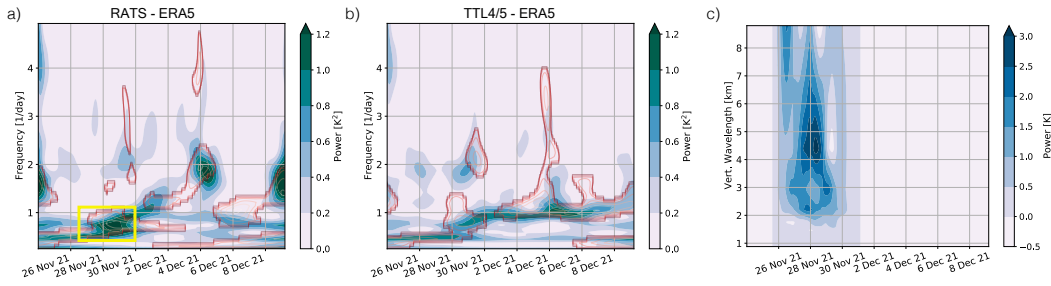


Figure 4. (a) Covariance of ERA5 temperatures between the two model levels that are closest to the balloon and RATS floating levels (blue and green contours). (b) Covariance of ERA5 temperatures interpolated to the TTL4 and TTL5 flight tracks. For both panels (a) and (b) the red contours identify where observed covariances $> 0.5K^2$ as presented in Fig. 2a and 3a. (c) ERA5 vertical wavelength spectrum for the wave packet for which the best agreement between measurements and ERA5 was found (yellow box in panel (a)). The spectra in a) and b) are shown as a function of time and wave frequency.

199 RATS is only about 200 m below the balloon. For the comparison with the observed TTL4
 200 and TTL5 covariances we use ERA5 data interpolated in space and time to the respec-
 201 tive balloon flight tracks.

202 Fig. 4a shows that for frequencies lower than 2 cycles/day the ERA5 simulated co-
 203 variances have similar structures and energies as the observed ones. This is especially
 204 true for the wavepacket observed on 29th November 2021 with a frequency of ~ 0.6 cycles/day
 205 (see yellow box in Fig 4a). This similarity gives confidence in the wave-packet analysis
 206 based on RATS observations, since the two figures Fig. 2a and Fig. 4a show correlations
 207 obtained with independent datasets. However, most of the ERA5 wave packets seem to
 208 evolve differently in time compared to observations and the observed high-frequency wave
 209 packets (29th November and 3rd December) are not resolved at all in ERA5.

210 For the wave packed that is well reproduced in ERA5 (yellow box in Fig 4a) we cal-
 211 culated the vertical wavelength for comparison with vertical wavelength estimates from
 212 RATS. For this analysis we interpolated ERA5 data on an equal-spaced vertical grid and
 213 then calculated the power spectrum of the vertical wavelength as a function of time (see

Fig. 4c). Most of the power is concentrated at a vertical wavelength of about 4.5 km which is similar to the estimated 5 km vertical wavelength derived from RATS observations.

Comparing the ERA5 and observed covariances of TTL4 and TTL5 (Fig. 4b) we draw similar conclusions. Again, for low frequencies, less than 1/day, there is similar power and temporal evolution, but the power for higher-frequency wave packets is underestimated in ERA5 and temporal evolution does not much resemble the observations. As ERA5 does not reproduce the observed packets that were well-resolved (~ 3 December in Fig. 4b), we do not attempt to compare the horizontal wavelengths between ERA5 and observations.

5 Conclusions & Discussion

In this study we present first results of a newly developed instrument RATS (Reel-down Atmospheric Temperature Sensor). RATS was developed during the second Strateole-2 campaign in 2021 and this study provides a proof-of-concept analysis of first measurements with this instrument. In its current design RATS was deployed about 200 m below the balloon gondola thus enabling observations of tropical waves with vertical wavelengths between ~ 400 m and 6 km. A previous study of long-duration balloon observations (Bramberger et al., 2022) found significant gravity waves with vertical wavelengths < 1 km. In the present case study, we observed tropical waves with vertical wavelengths between 1.5 km and 5 km. To extend the range of observable tropical waves future plans include the development of several RATS instruments allowing different vertical distances. These different RATS instruments can be deployed on several balloons in the next Strateole-2 campaign planned for late 2025.

The comparison to ERA5 reanalyses shows that the power distribution in the covariances at frequencies ≤ 1 cycle/day is similar to the observations, both for the RATS and the TTL4/TTL5 comparisons. However, the power is underestimated for high-frequency waves with frequencies ≥ 2 cycles/day, and some prominent observed higher frequency waves are absent in ERA5. Given the limited 10-day time series in this study, it is possible some higher frequency wave events may appear in ERA5 but with different timing than in the observations. The differences might be related to modeling limitations due to limited vertical resolution or differences in ERA5 representation of convection, which is the likely source of these tropical gravity waves (Corcos et al., 2021). Nevertheless, one low-frequency wave packet compared very well between ERA5 and RATS observations and we could therefore compare the respective vertical wavelengths. The found wavelengths agree well between ERA5 and RATS which adds confidence to the analysis technique applied to the RATS data.

Momentum fluxes calculated with a previously published method (Corcos et al., 2021) for the two high-frequency wave packets 1 and 2 in Fig. 2a are modest with about ~ 1 mPa and ~ 5 mPa, respectively. The found momentum fluxes are in concurrence with Corcos et al. (2021) where 1-5 mPa were the most commonly observed values and the global average momentum flux was ~ 5 mPa. In their study they found that collectively the high-frequency waves (> 1 cycle/day) contribute at least 25%, and possibly more than 50%, to the total force required to drive the QBO.

In general, there is good correspondence in the temperature covariance time series comparing the balloons to ERA5 for inertia-gravity waves with periods in the 1-2 day range. Similar signals were analyzed in ERA5 in detail over decades (Pahlavan, Fu, et al., 2021), and finding their contribution to forcing the QBO. Our comparison to these balloon data suggests these low-frequency gravity waves may be quite realistic in ERA5, both in their locations, timing, and amplitude (Fig. 4). However, although this is only a limited case study comparison, the ERA5 reanalysis appears to be deficient in gravity waves at higher frequencies. Additionally, ERA5 vertical resolution limitations were

264 implicated in missing waves seen in a previous balloon study (Bramberger et al., 2022)
 265 that should otherwise have been resolvable. Future comparisons between Strateole-2 bal-
 266 loon observations and reanalyses should further illuminate the strengths and limitations
 267 of the reanalysis datasets for representing tropical gravity waves.

268 Acknowledgments

269 The TSEN and RATS data were collected as part of Strateole-2, which is sponsored by
 270 CNES, CNRS/INSU and NSF. Joan Alexander and Martina Bramberger were supported
 271 by NSF grants 1642246 and 1642644. Development of FLOATS/RATS was supported
 272 by NSF award 1419932 and deployment was supported by NSF award 1642277. The au-
 273 thors would like to acknowledge Agustin Caro, the LATMOS gondola team, and Karim
 274 Ramage for their expertise and patience in the field. We give special thanks to Stephanie
 275 Venel and the CNES ballooning team for their exceptional balloon launches, profession-
 276 alism, and for making these difficult measurements possible.

277 References

- 278 Alexander, M. J. (2015). Global and seasonal variations in three-dimensional gravity
 279 wave momentum flux from satellite limb-sounding temperatures. *Geophys. Res.*
 280 *Lett.*, *42*(16), 6860-6867. doi: 10.1002/2015GL065234
- 281 Alexander, M. J., Gille, J., Cavanaugh, C., Coffey, M., Craig, C., Eden, T., ...
 282 Dean, V. (2008). Global estimates of gravity wave momentum flux from high
 283 resolution dynamics limb sounder observations. *J. Geophys. Res. Atmos.*,
 284 *113*(D15). doi: <https://doi.org/10.1029/2007JD008807>
- 285 Bramberger, M., Alexander, M. J., Davis, S., Podglajen, A., Hertzog, A., Kalnajs,
 286 L., ... Khaykin, S. (2022). First super-pressure balloon-borne fine-
 287 vertical-scale profiles in the upper ttl: Impacts of atmospheric waves on cir-
 288 rus clouds and the qbo. *Geophys. Res. Lett.*, *49*(5), e2021GL097596. doi:
 289 <https://doi.org/10.1029/2021GL097596>
- 290 Corcos, M., Hertzog, A., Plougonven, R., & Podglajen, A. (2021). Observation of
 291 Gravity Waves at the Tropical Tropopause Using Superpressure Balloons. *J.*
 292 *Geophys. Res. Atmos.*, *126*(15), e2021JD035165. doi: [https://doi.org/10.1029/](https://doi.org/10.1029/2021JD035165)
 293 [2021JD035165](https://doi.org/10.1029/2021JD035165)
- 294 Davis, S. M., Hegglin, M. I., Fujiwara, M., Dragani, R., Harada, Y., Kobayashi, C.,
 295 ... Wright, J. S. (2017). Assessment of upper tropospheric and stratospheric
 296 water vapor and ozone in reanalyses as part of s-rip. *Atmospheric Chemistry*
 297 *and Physics*, *17*(20), 12743–12778. doi: 10.5194/acp-17-12743-2017
- 298 Ern, M., Ploeger, F., Preusse, P., Gille, J. C., Gray, L. J., Kalisch, S., ... Riese, M.
 299 (2014). Interaction of gravity waves with the QBO: A satellite perspective. *J.*
 300 *Geophys. Res. Atmos.*, *119*(5), 2329-2355. doi: 10.1002/2013JD020731
- 301 Garfinkel, C. I., Gerber, E. P., Shamir, O., Rao, J., Jucker, M., White, I., & Paldor,
 302 N. (2022). A QBO Cookbook: Sensitivity of the Quasi-Biennial Oscilla-
 303 tion to Resolution, Resolved Waves, and Parameterized Gravity Waves. *J.*
 304 *Adv. Model. Earth Syst.*, *14*(3), e2021MS002568. Retrieved from [https://](https://agupubs.onlinelibrary.wiley.com/doi/abs/10.1029/2021MS002568)
 305 [agupubs.onlinelibrary.wiley.com/doi/abs/10.1029/2021MS002568](https://doi.org/10.1029/2021MS002568) doi:
 306 <https://doi.org/10.1029/2021MS002568>
- 307 Goetz, J. D., Kalnajs, L. E., Deshler, T., Davis, S. M., Bramberger, M., & Alexan-
 308 der, M. J. (2023). A fiber-optic distributed temperature sensor for continuous
 309 in situ profiling up to 2 km beneath constant-altitude scientific balloons. *At-*
 310 *mos. Meas. Tech.*, *16*(3), 791–807. doi: 10.5194/amt-16-791-2023
- 311 Haase, J., Alexander, M., Hertzog, A., Kalnajs, L., Deshler, T., Davis, S., ... Venel,
 312 S. (2018). Around the world in 84 days. *EOS*, *99*. doi: [https://doi.org/](https://doi.org/10.1029/2018EO091907)
 313 [10.1029/2018EO091907](https://doi.org/10.1029/2018EO091907)
- 314 Hersbach, H., Bell, B., Berrisford, P., Hirahara, S., Horányi, A., Muñoz Sabater,

- 315 J., ... Thópaút, J.-N. (2020). The ERA5 global reanalysis. *Quart. J. Roy.*
 316 *Meteor. Soc.*, *146*(730), 1999-2049. doi: <https://doi.org/10.1002/qj.3803>
- 317 Hertzog, A., Basdevant, C., Vial, F., & Mechoso, C. R. (2004). The accuracy
 318 of stratospheric analyses in the northern hemisphere inferred from long-
 319 duration balloon flights. *Q.J.R. Meteorol. Soc.*, *130*(597), 607-626. doi:
 320 <https://doi.org/10.1256/qj.03.76>
- 321 Holt, L. A., Lott, F., Garcia, R. R., Kiladis, G. N., Cheng, Y.-M., Anstey, J. A.,
 322 ... Yukimoto, S. (2020). An evaluation of tropical waves and wave forc-
 323 ing of the QBO in the QBOi models. *Q J R Meteorol Soc.*, *n/a*(n/a). doi:
 324 <https://doi.org/10.1002/qj.3827>
- 325 Jensen, E. J., Pfister, L., Jordan, D. E., Bui, T. V., Ueyama, R., Singh, H. B., ...
 326 Pfeilsticker, K. (2017). The NASA Airborne Tropical TRopopause EXper-
 327 iment: High-Altitude Aircraft Measurements in the Tropical Western Pacific.
 328 *Bull. Am. Meteorol. Soc.*, *96*, 129-143. doi: [doi:10.1175/BAMS-D-14-00263.1](https://doi.org/10.1175/BAMS-D-14-00263.1)
- 329 Kalnajs, L. E., Davis, S. M., Goetz, J. D., Deshler, T., Khaykin, S., St. Clair, A.,
 330 ... Lykov, A. (2021). A reel-down instrument system for profile measure-
 331 ments of water vapor, temperature, clouds, and aerosol beneath constant-
 332 altitude scientific balloons. *Atmos. Meas. Tech.*, *14*(4), 2635-2648. doi:
 333 [10.5194/amt-14-2635-2021](https://doi.org/10.5194/amt-14-2635-2021)
- 334 Kim, J.-E., & Alexander, M. J. (2015). Direct impacts of waves on tropical cold
 335 point tropopause temperature. *Geophys. Res. Lett.*, *42*(5), 1584-1592. doi: [10.1002/2014GL062737](https://doi.org/10.1002/2014GL062737)
- 336
 337 Kim, J.-E., Alexander, M. J., Bui, T. P., Dean-Day, J. M., Lawson, R. P., Woods,
 338 S., ... Jensen, E. J. (2016). Ubiquitous influence of waves on tropical
 339 high cirrus clouds. *Geophysical Research Letters*, *43*(11), 5895-5901. doi:
 340 <https://doi.org/10.1002/2016GL069293>
- 341 Kim, Y.-H., & Chun, H.-Y. (2015). Momentum forcing of the quasi-biennial os-
 342 cillation by equatorial waves in recent reanalyses. *Atmos. Chem. and Phys.*,
 343 *15*(12), 6577-6587. doi: [10.5194/acp-15-6577-2015](https://doi.org/10.5194/acp-15-6577-2015)
- 344 Pahlavan, H. A., Fu, Q., Wallace, J. M., & Kiladis, G. N. (2021). Revisiting the
 345 Quasi-Biennial Oscillation as Seen in ERA5. Part I: Description and Momen-
 346 tum Budget. *J. Atmos. Sci.*, *78*(3), 673 - 691. doi: [10.1175/JAS-D-20-0248.1](https://doi.org/10.1175/JAS-D-20-0248.1)
- 347 Pahlavan, H. A., Wallace, J. M., Fu, Q., & Kiladis, G. N. (2021). Revisiting the
 348 quasi-biennial oscillation as seen in era5. part ii: Evaluation of waves and
 349 wave forcing. *J. Atmos. Sci.*, *78*(3), 693 - 707. doi: <https://doi.org/10.1175/JAS-D-20-0249.1>
- 350
 351 Richter, J. H., Anstey, J. A., Butchart, N., Kawatani, Y., Meehl, G. A., Osprey,
 352 S., & Simpson, I. R. (2020). Progress in simulating the quasi-biennial
 353 oscillation in cmip models. *Journal Geophysical Research: Atmospheres*,
 354 *125*(e2019JD032362). doi: [10.1029/2019JD032362](https://doi.org/10.1029/2019JD032362)
- 355 Richter, J. H., Butchart, N., Kawatani, Y., Bushell, A. C., Holt, L., Serva, F., ...
 356 Yukimoto, S. (2020). Response of the Quasi-Biennial Oscillation to a warm-
 357 ing climate in global climate models. *Quart. J. Roy. Meteor. Soc.*, 1-29. doi:
 358 [10.1002/qj.3749](https://doi.org/10.1002/qj.3749)
- 359 Scaife, A. A., Baldwin, M. P., Butler, A. H., Charlton-Perez, A. J., Domeisen,
 360 D. I. V., Garfinkel, C. I., ... Thompson, D. W. J. (2022). Long-range pre-
 361 diction and the stratosphere. *Atmospheric Chemistry and Physics*, *22*(4),
 362 2601-2623. doi: [10.5194/acp-22-2601-2022](https://doi.org/10.5194/acp-22-2601-2022)
- 363 Solomon, S., Rosenlof, K., Portmann, R., Daniel, J., Davis, S., Sanford, T., &
 364 Plattner, G.-K. (2010, 03). Contributions of Stratospheric Water Vapor to
 365 Decadal Changes in the Rate of Global Warming. *Science*, *327*, 1219-23. doi:
 366 [10.1126/science.1182488](https://doi.org/10.1126/science.1182488)
- 367 Stockwell, R. G., Mansinha, L., & Lowe, R. P. (1996). Localization of the complex
 368 spectrum: the S transform. *IEEE Transactions on Signal Processing*, *44*(4),
 369 998-1001. doi: [10.1109/78.492555](https://doi.org/10.1109/78.492555)

- 370 Ueyama, R., Schoeberl, M., Jensen, E., Pfister, L., Park, M., & Ryo, J.-M. (2023).
371 Convective impact on the global lower stratospheric water vapor budget. *Jour-*
372 *nal of Geophysical Research: Atmospheres*, *128*(6), e2022JD037135. doi:
373 <https://doi.org/10.1029/2022JD037135>
- 374 Vincent, R. A., & Alexander, M. J. (2020). Balloon-Borne Observations of Short
375 Vertical Wavelength Gravity Waves and Interaction With QBO Winds. *J.*
376 *Geophys. Res. Atmos.*, *125*(15), e2020JD032779. doi: 10.1029/2020JD032779
- 377 Wilson, R., Pitois, C., Podglajen, A., Hertzog, A., Corcos, M., & Plougonven, R.
378 (2023). Detection of turbulence occurrences from temperature, pressure, and
379 position measurements under superpressure balloons. *Atmos. Meas. Tech.*,
380 *16*(2), 311–330. doi: 10.5194/amt-16-311-2023
- 381 Wright, C. J., Osprey, S. M., Barnett, J. J., Gray, L. J., & Gille, J. C. (2010).
382 High resolution dynamics limb sounder measurements of gravity wave activ-
383 ity in the 2006 arctic stratosphere. *J. Geophys. Res. Atmos.*, *115*(D2). doi:
384 <https://doi.org/10.1029/2009JD011858>